Progress in Nuclear Energy 137 (2021) 103740

Contents lists available at ScienceDirect

Progress in Nuclear Energy

journal homepage: http://www.elsevier.com/locate/pnucene

# Radiological characterisation in view of nuclear reactor decommissioning: On-site benchmarking exercise of a biological shield

Margarita Herranz [a,*], Sven Boden [b], Péter Völgyesi [c], Raquel Idoeta [a], Wouter Broeckx [b], Jesus Ruiz González [d], Polina Otiougova [e], Axel Klix [f], Lou Sai Leong [g], Zoltán Hlavathy [c], István Almási [c], Khalil Amgarou [h], Marielle Crozet [h], Fernando Legarda [a]

[a] UPV/EHU, University of the Basque Country, Spain
[b] SCK CEN, Belgian Nuclear Research Centre, Belgium
[c] MTA-EK, Hungarian Academy of Sciences Centre for Energy Research, Hungary
[d] Tecnatom, Spain
[e] PSI, Paul Scherrer Institute, Switzerland
[f] KIT, Karlsruhe Institute of Technology, Germany
[g] Mirion Technologies, France
[h] CEA, France

ARTICLE INFO

*Keywords:*
Radiological characterisation
D&D processes
Dose-rate measurements
Total gamma measurements
In-situ gamma-ray spectrometry

ABSTRACT

Nearly all decommissioning and dismantling (D&D) projects are steered by the characterisation of the plant being dismantled. This radiological characterisation is a complex process that is updated and modified during the course of the D&D. One of the tools for carrying out this characterisation is the performance of in-situ measurements.

There is a wide variety of equipment and methodologies used to carry out on-site measurements, depending on the environment in which they are to be carried out and also on the specific objectives of the measurements and the financial and personnel resources available. The extent to which measurements carried out with different types of equipment or methodologies providing comparable results can be crucial in view of the D&D strategy development and the decision-making process.

This paper concerns an on-site benchmarking exercise carried out at the activated biological shield of Belgian Reactor 3 (BR3). This activity allows comparison and validation of characterisation methodologies and different equipment used as well as future interpretation of final results in terms of uncertainties and sensitivities. This paper describes the measurements and results from the analysis of this exercise. Other aspects of this exercise will be reported in separate papers. This paper provides an overview of the on-site benchmarking exercise, outlines the participating organisations and the measurement equipment used for total gamma, dose rate and gamma spectrometry measurements and finally, results obtained and their interpretations are discussed for each type of measurement as a function of detector type.

Regarding the dose measurements, results obtained by using a large variety of equipment are very consistent. In view of mapping the inner surface of the biological shield the most appropriate equipment tested might be the organic scintillator, the BGO or even the ionisation chamber. In addition, for mapping this surface, the most appropriate total gamma equipment tested might be the $LaBr_3$(Ce), the thick organic scintillator or the BGO. These measurements can only be used as a secondary parameter in a relative way. Results for the gamma spectrometry are very consistent for all the equipment used and the main parameters to be determined.

## 1. Introduction

For the World Nuclear Association (WNA, 2019) decommissioning is defined as the permanent removal of a facility (e.g. reactor) from service, also the subsequent actions of safe storage, dismantling and making the site available for unrestricted use. Hence, decommissioning refers to

* Corresponding author. Nuclear Engineering and Fluid Mechanics dpt. – EI Bilbao (UPV/EHU), Pza. Ingeniero Torres Quevedo 1, 48013, Bilbao, Spain.
*E-mail address:* m.herranz@ehu.es (M. Herranz).

https://doi.org/10.1016/j.pnucene.2021.103740
Received 6 May 2020; Received in revised form 20 December 2020; Accepted 10 April 2021
Available online 28 April 2021

the administrative and technical actions taken to remove all or some of the regulatory controls from an authorized facility allowing reusing the site and/or the facility. The development of the initial site characterisation before the decommissioning of nuclear installations by taking a waste-led approach is essential in ensuring that decommissioning is accomplished in a safe and cost-effective manner.

The radiological characterisation process, which represents the determination of the nature, location and concentration of radionuclides in a nuclear facility (NEA, 2013), is a key element of the planning, controlling and optimising of decommissioning and dismantling (D&D) activities and relevant for shutdown nuclear installations, the buildings containing these nuclear installations and the related (nuclear) sites. Effective characterisation allows the extent and nature of the contamination to be determined, thus providing necessary information to support facility dismantling, the management of waste arising (IAEA, 2004; IAEA, 2007), the protection of workers, of the public and the environment, and associated cost estimations (IAEA, 1998a; IAEA, 1998b).

An initial facility/site characterisation generally consists of a collection of historical data, on-site measurements and sampling combined with off-site non-destructive and destructive analysis (IAEA, 1998a; NEA, 2017). All data acquired needs to be validated, analysed, coupled and interpreted in a way that reliable decisions for the further decommissioning process can be made.

In 2015, 156 reactor power plants (RPP) worldwide were stopped or under D&D operations. By 2050 more than half of the present 400 GW nuclear capacity around the world is already scheduled to be shut down for dismantling. In Europe, this will result in a volume increase of radioactive waste while the current storage sites have a limited capacity. In addition, handling, treatment, storage, transportation and disposal of radioactive waste also present social issues. In most cases, only 20% of D&D waste are radiation emitting materials compared to the huge limitation of disposal capacity in terms of volume, radiological acceptance and waste composition with regards to cost, deadlines and safety. More precise characterisation data are an essential part of the definition of radioactive waste helping to its classification and categorization.

Progress in developing innovative approaches and technologies in this domain should contribute to identifying potential gains compared to the substantial investment required to decommission existing nuclear facilities. It is essential to act on the early stages of the dismantling for the management of all radioactive waste. Nuclear materials are a complex issue considering the wide variety of matrices and contaminants, therefore, proper radiological and chemical characterisation of plant areas becomes a primary technical focus and a necessary precondition for a successful project regarding the definition of viable dismantling scenarios and the classification and segregation of the different contaminated materials. Characterisation data are also an essential part of the decommissioning cost estimation process.

In this context, the EURATOM work program project INSIDER (Improved Nuclear SIte characterisation for waste minimization in Decommissioning under constrained EnviRonment) aims at improving the management of contaminated materials arising from decommissioning and dismantling (D&D) operations (INSIDER, 2017). The project develops and validates an improved integrated methodology of characterisation based on different new statistical processing and modelling helping the definition of the sampling program, coupled with present (and adapted) analytical and measurement methods, both on-site and in-lab, with respect to the sustainability and economic objectives described in the previous paragraphs. The INSIDER strategy is being validated on the three different use cases (Peerani et al., 2018).

- Radioactive liquids and sludges stored in tanks at an R&D facility;
- The activated biological shield of a reactor facility; and
- Contaminated soils as a result of an accident.

This paper only concerns the on-site benchmarking exercise performed at the activated biological shield of the Belgian Reactor 3 (BR3). The operator had developed and implemented a specific radiological characterisation programme, applying the overall strategy established within the INSIDER project. After, the on-site benchmarking exercise was developed by measuring in some of the points where the statistical processing and modelling had been applied; finally an interlaboratory comparison exercise on reference and real samples, taken at the same points where the on-site measurements were performed are under development. These benchmarking exercises are complementing activities within the global project that allow us to check not only the validity of the data obtained through the numerical simulation, but also the consistency between some of the results obtained in the laboratory and on-site. Also these on-site benchmarking exercise can be used in the comparison of the different performances of some of the equipment usually used by the different companies and institutions to carry out these type of on-site measurements. The latter allows future interpretation of final results in terms of uncertainties and sensitivities. Thus, all these data will contribute to the proper radiological characterisation of the facility and therefore to the definition of the materials as waste or released materials and to the categorization of radioactive waste, which are the main objectives of the general project.

This paper describes the measurements and results from the analysis of the on-site benchmarking exercise, as one of its objectives is the test, verification and assessment of three in situ characterisation techniques (dose rate, total gamma and radionuclide distribution via gamma spectrometry) through the use of different commercially available instrumentation. The goal is to check as many ad hoc instruments as possible. Other aspects of this exercise will be reported in separate papers. Section 2, regarding the methodology, summarises the use case and provides an overview of the measurement programme of the on-site benchmarking exercise. Section 3 outlines the participating organisations and describes the measurement equipment used. Results obtained and their interpretations are discussed for each type of measurement as a function of detector type in section 4, followed by the conclusions for the on-site benchmarking exercise.

## 2. Methodology

### 2.1. The BR3 biological shield

This benchmarking exercise was accomplished during the last quarter of 2018, by performing various radiological measurements in the biological shield of the BR3 reactor, located in the SCK CEN (Mol, Belgium). The 40 MW pilot Pressurised Water Reactor (PWR) was brought into operation in October 1962 and was definitively shutdown in 1987, after 25 years of operation and eleven campaigns. The heart of the reactor, the reactor pressure vessel and primary circuit, were located in the reactor building. Today, all the main installations have been dismantled. The total volume of the biological shield, consisting of reinforced high-density concrete, and considered to be potentially activated by neutrons is about 600 $m^3$. The wall thickness is about 1.2 m. Fig. 1 shows a 3D model of the reactor pit and a picture of the platform installed into the reactor pit for having access to the inner pool walls. Point A, B and C represent the points were the in-situ measurements are carried out.

The main goal of the BR3 biological shield radiological characterisation program consists of an economic optimisation of the biological shield dismantling strategy, using a waste-led approach. In order to reach this main goal, the SCK CEN established three sub objectives (Boden et al., 2018, 2019):

- Create a 3D specific activity distribution map;
- Quantify and localize the different end-stage volumes; and
- Economically optimise volumes in view of a waste-led approach.

Pre-existing data such as neutron activation calculations and initial sampling radiological characterisation were used as basic input for the

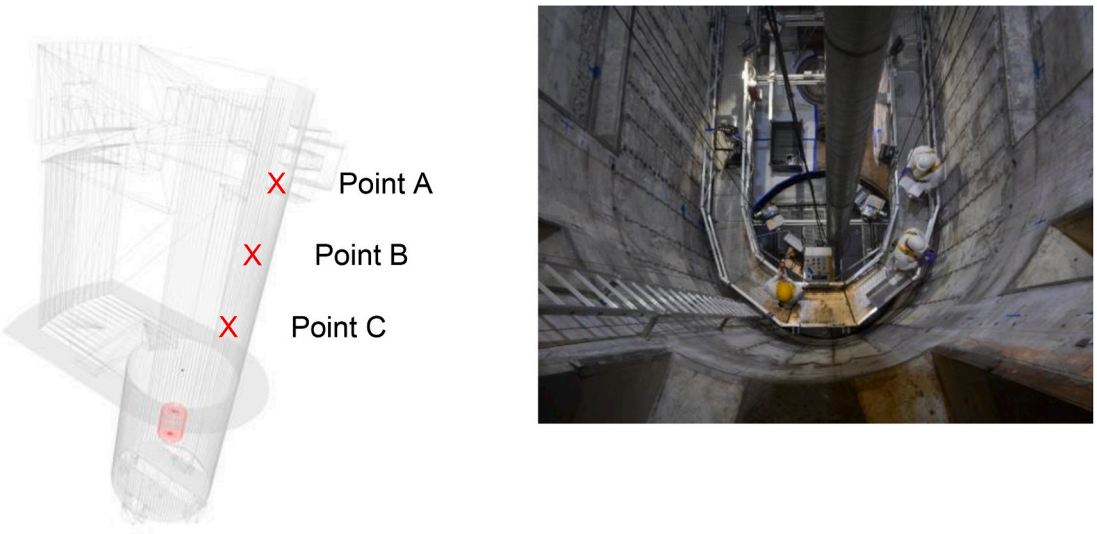


**Fig. 1.** 3D model of the reactor and neutron shield tank pit (left). The red cylinder indicates the position of the reactor fuel during operation. Picture of the platform installed into the reactor pit after removal of the pool liner (right).

sampling design. The overall operator sampling and analysis programme consisted of total gamma measurements at the inner surface of the biological shield (secondary data) and gamma spectrometry measurements on drill core samples (primary data). The characterisation program showed the presence of the following radionuclides in the concrete and reinforcement: H-3, C-14, Ca-41, Fe-55, Co-60, Ni-63, Ba-133, Cs-134, Cs-137, Eu-152, Eu-154 and Eu-155 (Boden et al., 2019; Broeckx et al., 2020). Radionuclides with low occurrence and relatively short-lived nuclides (Fe-55, Cs-134, and Eu-155) are nearly all decayed and difficult to measure nuclides (C-14, Ca-41, Ni-63) are specifically being examined in the sample interlaboratory and benchmarking exercises. The essential beta/gamma emitters for the in-situ benchmarking exercise were basically limited to the activation products Eu-152, Ba-133, Co-60 and Cs-137 for potential traces of contamination. Therefore, the gamma ray energy range to be measured in this intercomparison campaign is up to 1408 keV.

At the moment of the benchmarking exercise, the expected activity concentration level of the main radionuclide being present in the biological shield ranged from below 0.1 $Bq.g^{-1}$ on top of the biological shield, up to a maximum of 50 $Bq.g^{-1}$ at the level close to the highest neutron flux during operation. The expected contact dose rate ranged from natural background level (about 0.7 $\mu Sv.h^{-1}$) up to 10 $\mu Sv.h^{-1}$. Potentially existing constraints (Aspe and Idoeta, 2019; Aspe et al., 2020), were mainly related to typical nuclear safety issues (radiation & contamination hazards) but above all to access limitations and classical safety hazards.

### 2.2. On-site benchmarking programme

The overall radiological characterisation for the BR3 biological shield is based on total gamma measurements at the inner surface of the biological shield (secondary data) and gamma spectrometry measurements on drill core samples (primary data) (Boden et al., 2019). The uncertainties related to the measurements of drill core samples are tackled within the INSIDER project by performing specific interlaboratory comparison exercises on real and reference samples. For the on-site benchmarking exercise described in this paper, we therefore focussed on the gamma based measurements that could be directly performed on the inner surface of the biological shield. As a starting point for the on-site benchmarking exercise, we considered two types of relatively simple, commonly used, fast, easy and straightforward measurement methods: dose rate and total gamma. Additionally we examined the feasibility to use in-situ gamma spectrometry in this stage of the characterisation process.

In this benchmark exercise there is no reference value for the measured parameters, so the true value is unknown. In fact, only for gamma-spectrometry there are some indicative values. Dose rate and total gamma values are strongly dependent on the characteristics of the reference source used to calibrate the detector and those characteristics were fixed in the exercise instructions. Thus, we are testing precision, not accuracy.

Therefore, one of the objectives of this exercise is to test various commercially available instrumentation to carry out dose rate, total gamma and gamma-spectrometry, checking their ability to provide comparable results. The goal is to check as many of the instruments as possible from among those commonly used and described in deliverable 5.1 of this INSIDER project (Amgarou et al., 2018).

In order to cover the full range of activity concentration levels for the biological shield, we selected three fixed points to perform dose rate and total gamma measurements (See Fig. 1):

- Point A, at the top of the reactor pool (relative low activation levels),
- Point B, approximately at medium height in the reactor pool (relative medium activation levels), and
- Point C, close to the bottom of the reactor pool and therefore close to the maximum activation levels.

These points were literally drawn on the wall, being the same for all the participating teams and situated in the center of a 1 × 1 m square to help to position the instruments. See Fig. 2.

For both dose rate and total gamma measurements, five sets consisting of five consecutive measurements each (in order to test repeatability) were carried out for each of the three points. Between every set, the equipment was removed and repositioned (in order to test reproducibility). This resulted in a total of 25 single dose rate and total gamma measurements for each point. We chose to use a distance between source and detector near zero (i.e. direct contact) and a straightforward open collimation (detector neither shielded nor collimated). In order to be able to compare the results acquired by each measurement team, we agreed to calibrate the dose-rate probes in terms of ambient gamma dose equivalent rate H*(10) (in $\mu Sv.h^{-1}$) using Cs-137 reference sources. Since no reference for total-gamma probes is existing, we decided that each measurement team should calibrate their probe using a Cs-137 point source provided by the SCK CEN. The probes were positioned perpendicular to the centre of the 1 × 1 m squares shown in Fig. 3.

**Fig. 2.** Picture of the point C, and its associated square, during the gamma spectrometry measurements, in the bottom of the reactor pool.

The in-situ gamma spectrometry measurements were limited to point C, due to timing constraints. Each team used their own positioning and collimation system as well as their own measuring probes. Nevertheless, all of them had to follow the instructions to be able to collect the radiation coming from a circular surface of 30 cm in diameter, centered on point C and a 30 cm of distance.

The instructions provided to each team were the following:

- Background and side detector shielding should be applied;
- Two separate measurements should be performed to correct for the background: one measurement using an open 90° collimation and one measurement with closed collimation at the front of the detector;
- The detector should be pointed towards point C with a 30 cm distance between the detector and the pool wall; and
- If possible, a long data acquisition time (e.g. overnight) should be used.

All measurement teams used their own equipment, usually efficiency-calibrated by using punctual or volumetric homogeneous sources; however, in this exercise, the source to be measured was a large and not homogeneous volume. Therefore, to obtain the specific calibration for this source each team used their own calibration procedure; typically based on Monte-Carlo modelling codes. These calculation codes are used to simulate both the detector and the biological shield to obtain the detector response to a specific source. So, not only the geometrical structure and compositions of the different elements of the detector and its collimation system, are needed, but also the geometrical, physical and chemical characteristics of the biological shield (such as the chemical composition and density of the concrete), the standard activation profile parameters of the radionuclides we are looking for in the shield (i.e. ratio of the activity concentration at the surface compared to the maximum activity concentration, depth of the maximum activity concentration, relaxation length) and the source-to-detector relative position. By using this data, the theoretical spectrum for one $Bq.g^{-1}$ of each radionuclide is obtained and by comparison to the obtained experimental spectrum the amount of $Bq.g^{-1}$, for each radionuclide, in the biological shield is obtained.

So, the SCK CEN provided all facility pre-defined parameters, not only consisting of the basic model parameters, but also the standard activation profile parameters. In principle, advanced calculation methods using high purity germanium detectors should allow estimation of these parameters (Boden and Cantrel, 2007). Nevertheless, we predetermined that such an exercise would be too complex taking practical considerations into account, such as the use of different types of detectors (high and medium resolution) and the fact that the high density concrete was covered by a screed normal concrete layer with different chemical composition and density and also because of the existence of other common structural components in real installations like this one.

Under all these conditions, the measurement teams were expected to report on the following parameters:

- Depth where Ba-133 $\leq$ 0.1 $Bq.g^{-1}$;
- Depth where Eu-152 $\leq$ 0.1 $Bq.g^{-1}$;
- Depth where $\Sigma$(Ba-133/0.1 + Eu-152/0.1) $\leq$ 1 $Bq.g^{-1}$;
- Activity ratio Eu-152/Eu-154; and
- Cs-137 surface activity concentration (in $Bq.cm^{-2}$).

## 3. Participating organisations & measurement equipment used

### 3.1. Participating organisations

Due to space and time constraints, only 7 measurement teams from the following seven different organisations participated in this on-site benchmarking exercise (alphabetical order):

- KIT, Karlsruhe Institute of Technology (Germany)

**Fig. 3.** Pictures of the point B, and its associated 1 × 1 m square, with some dose rate and total gamma probes perpendicularly situated at the required distance.

- Mirion Technologies (France)
- MTA-EK, Hungarian Academy of Sciences Centre for Energy Research (Hungary)
- PSI, Paul Scherrer Institute (Switzerland)
- SCK CEN, Belgian Nuclear Research Centre (Belgium)
- Tecnatom (Spain)
- UPV/EHU, University of the Basque Country (Spain)

### 3.2. Measurement equipment used

The strategy of this benchmarking exercise for on-site measurements was to check, as much as possible, the equipment typically used for these type of measurements (Amgarou et al., 2018). Considering the limitations of accessibility to the facility (only 6 measuring teams were allowed to participate) and the resources of the teams involved in the campaign, we chose the most conventional equipment.

The overview of measurement equipment is described for each of the measurement types performed within the BR3 on-site benchmarking exercise:

- Dose rate;
- Total gamma; and
- In-situ gamma spectrometry.

This chapter contains a specific paragraph for the response of various detectors as a function of photon energy, due to its importance in the case of total signal interpretations.

#### 3.2.1. Dose rate

All participating organisations carried out the dose rate measurements using their own selected equipment. Table 1 gives an overview of the properties of the equipment used. Four typical but different detector principles were used: an ionisation chamber, a proportional counter, Geiger-Müller counters and scintillators.

Considering the three types of gas-filled detectors with the same detector size, the least sensitive detector is the ionisation chamber, where there is no gas amplification. For the ionisation chamber, the pulse size is equal to the number of ion pairs produced directly by the radiation. A proportional counter of the same dimension is considered to be more sensitive, since some gas amplification is taking place. The Geiger-Müller tube is the most sensitive gas filled detector, because it has the largest pulse size and each radiation will produce an avalanche of ion pairs.

The solid scintillator detectors have a higher density and a higher effective atomic number than gas filled detectors. Therefore, scintillation detectors of a similar size as gas-filled detectors would be more sensitive to lower activity levels (Knoll, 2010). Inorganic scintillators, compared to the organic ones, are supposed to have very good efficiencies, given their high atomic number and density, but can overestimate the dose at low energies, depending on the calibration used.

The low limits of the energy operational range are quite similar for all the equipment used although some can be sensitive to X-rays coming from the radionuclides detected; some differences appear in the high limit. However, considering the expected percentage of gamma emissions for a typical radionuclide composition of the BR3 biological shield, only 5% of the gamma emissions could have been potentially missed by some of the tools used. See section 3.2.3. for more details.

In terms of user-friendliness, all equipment used is fairly simple and straightforward. An additional important difference between detectors might be the response time. The manufacturer of the ionisation chamber reports a response time of 5 s, while the manufacturer of the Geiger-Müller (Model: Telepole) indicates a response time of 30 s. It is just matter of taking into account the response time of the equipment when performing measurements.

Some teams used the standard calibration conversion performed by the manufacturer. Others provided a specific calibration performed by a recognised Metrology lab (Ionisation chamber, organic scintillator and BGO scintillator). In addition, it must be mentioned that The 6150AD-t teletector probe was calibrated for so-called “Photon equivalent dose Hx” (GfdT, 2002), instead of “Ambient dose equivalent (H*(10))”. According to the internal communication with the calibration laboratory at PSI, the Hx can differ from H*(10) up to 5%. For Cs-137 The H*(10)/Hx = 1.05 (Steffen, 2020).

It must be noticed that for some equipment, the lowest value of the calibration range might be above the lowest dose rate point finally measured at one point.

**Table 1**
Overview of the equipment properties used by the participants for the dose rate measurements (NP = not provided).

| Detector type | Gas | | | | Scintillator | | |
|---|---|---|---|---|---|---|---|
| Detector principle | Ionisation chamber | Proportional counter | Geiger-Müller | Geiger-Müller | Organic | CsI (Tl) | BGO |
| Brand | Fluke | Thermo Scientific | Rotem | Automess | Automess | Mirion | Own design |
| Model | 451P-DE-SI-RYR | FH40 G-L10 | Telepole | 6150 AD-t coupled with 6150 AD 6/H | 6150AD-b | Colibri-VLD | BGO |
| Operational range (μSv. $h^{-1}$) | 0–50000 | 0.01 – 1E+05 | 0.5 – 1E+06 | 0.5–9.99E+06 | 0.005–100 | 0.01–1000 | 0.01–1000 |
| Operational range (keV) See section 3.2.3. | 25–2000 | 30–4400 | 70–1100 | Low range tube: 65–1300 High range tube 65–3000 | 23–7000 | 59–1500 | 45–2000 |
| Calibration | H*(10) horizontal radiation bundle with Cs-137 according to ISO 4037 by Metrology lab | H*(10) conversion calibration by manufacturer | H*(10) conversion calibration by manufacturer | Hx Photon Equivalent calibration by manufacturer (classical quantity Hx) | H*(10) horizontal radiation bundle with Cs-137 according to ISO 4037 by Metrology lab | H*(10) ambient gamma dose equivalent rate by manufacturer (according to ICRP-60) | H*(10) horizontal radiation bundle with Cs-137 according to ISO 4037 by Metrology lab |
| Calibration date | 2018-06-01 | NP | NP | NP | 2018-10-08 | 2018-06-14 | 2018-09-25 |
| Calibration range (μSv. $h^{-1}$) | 3–30000 | NP | NP | NP | 3–70 | 0.15–360 | 0.8–10 |
| Response time (s) | 5 | 2–60 (depending on dose rate) | 30 | 5–30 | 10 | na | 60 |

### 3.2.2. Total gamma

Also in the case of total gamma measurements, each of the participants used their own equipment. In this case, only two measurement principles have been used: two gas – filled proportional counters and six scintillators. In the same way as for the dose rate measurements, the solid scintillator detectors have a higher density and higher effective atomic number compared to gas filled detectors. Therefore, scintillation detectors of a similar size as a gas-filled detector will be more sensitive to lower activity levels of the radiation being measured. As shown in Table 2, detector shapes, sizes and therefore surface to length ratios differ enormously.

Most of the other detectors were common gamma probes, not specifically designed for surface monitoring. Some of them were shielded by their own structure from beta rays potentially coming from radionuclides in the walls. It should also be pointed out that the operational gamma and X-ray ranges are slightly different for each of the different probes, due to their different configuration and manufacturing. Therefore, when considering the amount of X and gamma-rays coming from the source due to the essential emitters expected (Co-60, Ba133, Eu152 and Cs-137), different responses are expected from the different probes.

Three of the scintillator detectors (Berthold ZnS, Nuvia ZnS and Nuvia Organic) were standard surface contamination monitors. Two of them are designed for the measurement of mainly alpha and beta contamination (Berthold ZnS and Nuvia ZnS), consisting of a very thin and large surface ZnS detector and additionally an organic plastic scintillator in the second case. Due to their thin detector crystals, the sensitivity for gamma radiation is relatively low and therefore the detection limit might be sufficiently large compared to their abilities to detect beta radiation. Nevertheless, such detectors can be used for the detection of gamma radiation bearing in mind that the detector should be shielded from beta radiation, as in the case of the Berthold scintillator, with a metallic plate put on top of it to avoid detection of beta radiation. The large surface organic scintillator detector, Como 300G, has been specifically designed for measuring in-situ gamma radiation in building structures. It is equipped with an aluminium cover to shield it from beta radiation and the detector crystal is 20 mm, thicker than the other surface contamination monitors.

Regarding the other scintillators, the BGO detector used for this exercise, although very suitable for gamma rays detection, is relatively small and has a larger surface compared to its thickness. The two remaining medium resolution gamma scintillators used, NaI(Tl) and $LaBr_3$(Ce), also with high sensitivity to gamma rays, have a diameter that is equal to its thickness. For the latter, results were derived from summing up the counts registered along the whole gamma ray spectrum as it was connected to a multichannel analyzer. All these detectors are housed in aluminium that shields them for beta radiation.

Even the proportional counters considerably differ from each other in size: in one case the detector used is the same as for the dose rate measurements (Thermo scientific FH40 G-L10) with a 4.9:2.58 surface to length ratio while, in the other case, it is an equipment containing a detector with a very small surface compared to its length. They are both portable photon dose rate meters that have an output in terms of total count rate registered.

For the total gamma measurement, the total count rate signal was recorded. In order to be able to compare the results, we agreed in advance that each team should calibrate each detector with the same Cs-137 point source (measurement in contact) and that each team should report the results expressed as Cs-137 equivalent Bq per detector surface area ($cm^{-2}$).

The main difference with the dose rate measurements is the data acquisition time. Dose rate measurements typically consist of prompt measurements (taking into account the value of the response time). For the total gamma measurements, the data acquisition is usually integrated over a certain time period. There can be a certain impact on the results reported if the acquisition time was smaller than the response time.

### 3.2.3. Gamma tools response as a function of photon energy

The most important radionuclides being present in the BR3 biological shield in the order of concentration levels and contribution to acceptance criteria for unconditional and conditional release are Ba-133 and Eu-152, and Co-60 as a minor component. Fig. 4 shows the expected percentage of photon emissions for a typical radionuclide composition of the bulk concrete of the BR3 biological shield. The amount of photon emissions with an energy:

- between 30 and 50 keV is the most abundant;
- between 250 and 500 keV is very important;
- between 50 and 250 keV is important;
- above 1000 keV is limited; and
- between 500 and 1500 keV is nearly negligible.

There are also some X-rays with energies below 10 keV; however, their penetration in concrete is lower than 1 mm, so we can conclude that those photons will not reach the detector and therefore they are not considered in Fig. 4.

However, the expected X/gamma rays spectrum from the biological shield is expected to be strongly different from the one shown in Fig. 4, not only due to the dependence on the self-absorption in concrete but also to the different distribution of the radionuclides. In addition, the structural design of the wall should affect the expected percentage of gamma emissions shown in Fig. 4 by disturbing the X/gamma rays differently at every point (i.e. the presence of an outer layer of concrete with different density and characteristics than those of the bulk one, where the radionuclide composition of the main radionuclides is completely different). Then, the real X/gamma ray spectrum reaching

**Table 2**
Overview of the equipment properties used by the participants for the total gamma measurements.

| Detector type | Gas | | Scintillator | | | | | |
|---|---|---|---|---|---|---|---|---|
| Detector principle | Proportional counter | Proportional counter | ZnS | ZnS + organic | Organic | NaI(Tl) | $LaBr_3$(Ce) | BGO |
| Brand | Berthold | Thermo Scientific | Berthold | NuviaTECH instruments | NuviaTECH instruments | Mirion | Mirion + Hamamatsu | Own design |
| Model | LB 1236 | FH40 G-L10 | LB124 | Como 170 | Como300G | SG2R | $LaBr_3$ 1,5 “ | BGO |
| Detector shape | cylindrical | cylindrical | rectangular | rectangular | rectangular | Cylindrical | Cylindrical | cylindrical |
| Detector size (cm) | 3.4 × 11 | 2.5 × 2.58 | 24 × 14.2 x 1.1 | 24 × 13 x 0.1 | 24 × 13 x 2 | 5.08 × 5.08 | 3.81 × 3.81 | 1.485 × 0.8 |
| Surface ($cm^2$) | 9.1 | 39.9 | 341.0 | 312.0 | 312.0 | 20.3 | 11.4 | 1.7 |
| Volume ($cm^3$) | 99.9 | 25.3 | 34.5 | 31.2 | 624.0 | 103.0 | 43.4 | 1.4 |
| Acquisition time (s) | 45 (A,B) 30 (C) | 30, 60 | 30 | 20 | 15 | 20 | 30 | 60 |
| Operatinal range, keV. See section 3.2.3. | 30–1300 | 30–4400 | See Fig. 4 | See Fig. 4 | See Fig. 4 | 40 -1500. | 20–2800 | See Fig. 4 |

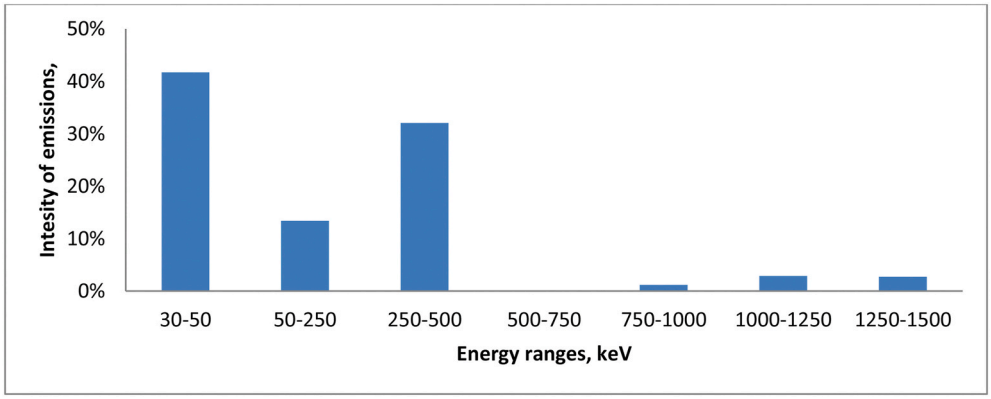


**Fig. 4.** Expected gamma emissions for a typical radionuclide composition of the BR3 biological shield (reference date 2020-01-01).

the detector at each of the measurement points is not well defined and neither is the response of the different probes.

Taking this into account, it is reasonable to consider that the response of the different probes will be different depending, among other things, on the response of the probes to the photon energy.

In this context, Figs. 5 and 6 present the relative detector response to Cs-137 as a function of photon energy for the equipment used in the BR-3 on-site benchmarking exercise for the dose rate measurements and total gamma measurements, respectively. This data has been provided by the manufacturers of the different probes or by the users of them.

As shown in Fig. 5, the BGO scintillator has a non linear response with respect to energy, but this nonlinearity with energy was corrected from the signal measured in order to report correct dose rate values. Equipment with other scintillators, organic and CsI(Tl) as well as ionisation chamber and proportional counter based equipment have a rather flat response to energy, typical for equipment intended for measuring the ambient dose rate with wide energy operational range and a response slightly different from 1 for energies below 100 keV. The most unusual response with energy is that from both GM dose rate meters (Rotem and Automess): their response to energies below 100 keV is too low and the particular response from Rotem equipment at high energies is extremely large.

For photon energies higher than 660 keV all the probes show a flat response, as shown in Fig. 6. However, for lower energies, their behaviour is quite different, the proportional counters (Berthold and Thermo) being the ones that show the most homogenous response as a function of energy as both are energy compensated proportional counters designed to provide ambient gamma dose equivalent rate. The thick organic scintillator from Nuvia, also has a relatively stable response in the energy region (250–500 keV) although it loses efficiency linearly for energies below 250 keV. At very low photon energies, its low efficiency response is also due to the aluminium cover used to shield it from beta radiation. The BGO used for these total gamma measurements is less sensitive to lower energy photons than the three other inorganic scintillators, ZnS, NaI(Tl) and $LaBr_3$(Ce), which are strongly energy dependent at low photon energies, strongly increasing its efficiency for energies lower than 600 keV.

It is clear that these kind of detector response differences can play an important role in the interpretation of the total gamma measurements.

### 3.2.4. *In-situ gamma spectrometry*

As well for the in-situ gamma spectrometry measurements, each team used their own equipment, likewise their own calculation methodologies, which includes the selection of the gamma lines to be taken into account for the radionuclides assessment. Table 3 lists both detectors and modelling tools. In addition, in this case, we observe a distinct diversity in detector types and sizes as well in the use of calculations codes. Two teams used medium resolution detectors being compact since no cooling of the detector crystal is needed; a $LaBr_3$(Ce) scintillator and a small CZT detector. All other teams used High Purity Germanium detectors of which three were traditionally cooled with liquid nitrogen and one (HPGe B2830, "Falcon") was electrically cooled.

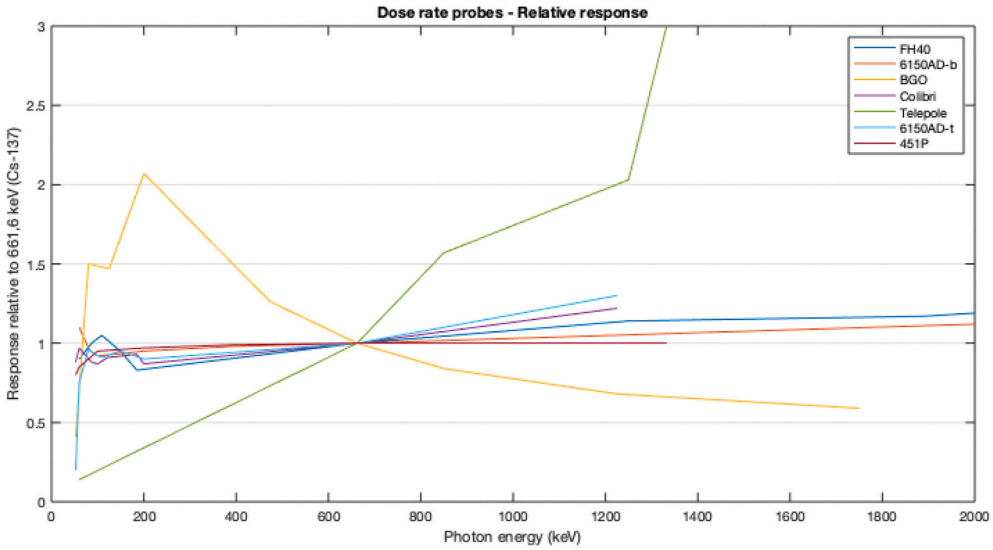


**Fig. 5.** Dose rate probes. Detector response relative to 661.6 keV (Cs-137) as a function of photon energy.

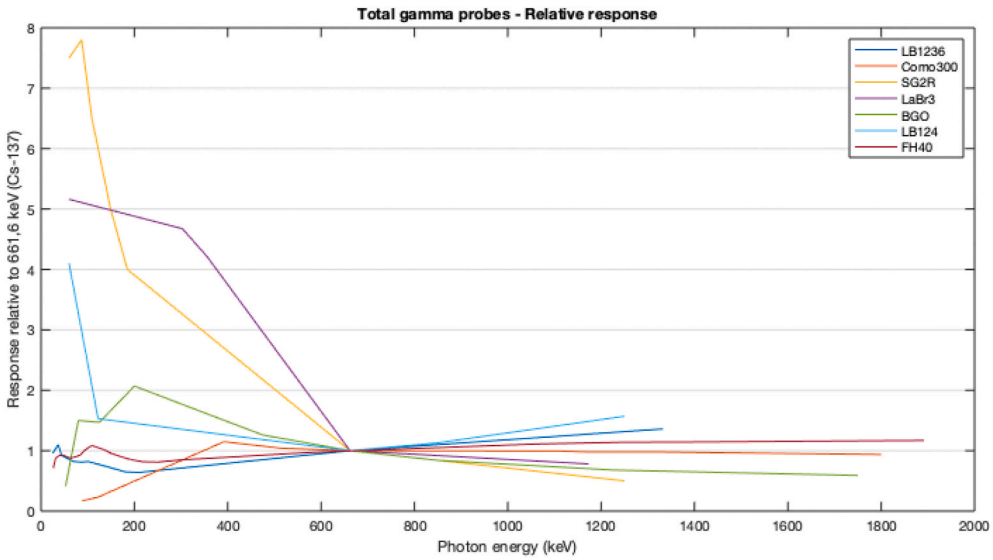


**Fig. 6.** Total gamma probes. Detector response relative to 661.6 keV (Cs-137) as a function of photon energy.

**Table 3**
Overview of the equipment properties used by the participants for the gamma spectrometry and calculations.

| | | | | | | |
|---|---|---|---|---|---|---|
| Detector type | Scintillator | Semi-Conductor | | | | |
| Detector resolution | Medium | Medium | High Resolution | | | |
| Crystal type and model | $LaBr_3$(Ce) 1.5"×1.5" | CZT 1 $cm^3$ | HPGe BE2830 | HPGe GL2020 | HPGe GX4018 | HPGe BE3830 |
| Manufacturer/Product | Mirion + Hamamatsu | Kromek | Mirion/Falcon | Mirion | Mirion | Mirion |
| Calibration & modelling | MCNP6.1 | PENELOPE MC | ISOCS | MCNP5-1.60 | ISOCS | ISOCS |
| Surface seen using 90° collimation ($m^2$) | 0.28 | 0.36 | No collimator 360° | 0.38 | 0.4 | 0.28 |
| Acquisition time (s) for open collimation | 60470 | 61200 | 61800 | 19492 | 54000 | 60000 |

The energy range covered by all of them is rather similar, although some of them are particularly suited for low energy gamma ray spectrometry (HPGe GL2020) and the other HPGe detectors cover low energy part. Regarding efficiency, all of them have more or less the same density but CZT and $LaBr_3$(Ce) have around 50 effective atomic number, larger than 32 of Ge. Given the data from detectors, the higher efficiency detectors would be $LaBr_3$(Ce) and HPGe GX4018. Given its low volume, the CZT is the one with the lowest efficiency.

For the modelling and calculations, three teams used the detector calibration and ISOCS (In Situ Object Counting System) of Mirion, while the other teams employed MCNP and Penelope Monte Carlo calculation codes.

An important remark is that one team did not comprehensively follow the instructions defined in advance: the Falcon detector used was not equipped with a collimator nor background shielding.

## 4. Results & interpretation

The results of the BR-3 on-site benchmarking exercise have been analysed following the appropriate state-of-the-art techniques being applied for interlaboratory exercises (e.g. ANOVA). This specific analysis and interpretation will be described in a separate paper. In the current paper, we concentrate on the description of the results obtained by using the different measurement equipment in view of accomplishing the general benchmarking exercise goal for testing, verifying and assessing in situ measurement equipment for those three in situ characterisation determinations (dose rate, total gamma and gamma spectrometry radionuclide analysis).

In this exercise, systematic uncertainties that could arise from differences between the real source, the biological shield, and the calibration one, the non-uniform distribution of radionuclides within the shield, the non-uniform density or chemical composition of the materials in this shield and the differences, among the different measuring teams, in the shield-to-detector distance, do not have any effect in the comparison of the results. All the teams used the same values for all these parameters.

### 4.1. Dose rate measurement results

Table 4 shows the dose rate results obtained for the various measurement equipment used. The values reported correspond to the arithmetic mean of the 25 single measurements for each of the points A, B and C. The reported expanded uncertainty (coverage factor 2) consists of the standard deviation of the measured values and the uncertainty on the detector calibration; other potential sources of uncertainty are not taken into account. Of course, no reference values are available to compare the results with each other.

The mean dose rates measured are relatively low with roughly only one magnitude order of difference: 0.31–3.4 $\mu Sv.h^{-1}$. It is important to mention that some of the values measured are below the operational measurement range reported by the manufacturer (see Table 1). This is the case for measurement points A and B for the Geiger-Müller counters. Since the measured values are relatively low, in most cases, the measured values are below the range of the real calibration performed. This is, for instance, the case for the organic scintillator and for the ionisation chamber, where the lowest calibrated Cs-137 equivalent gamma dose rate H*(10) was 3 $\mu Sv.h^{-1}$. This means that the uncertainty on the results for A and B might be underestimated due to an extrapolation of the efficiency curve.

Fig. 7 shows a graphical representation of the results reported in Table 4. We observe the following:

**Table 4**
Dose rate results (μSv.h$^{-1}$) for the various measurement equipment used and expanded uncertainty (relative uncertainty between brackets, k = 2).

| | Ionisation Chamber | Proportional Counter | Geiger-Müller | | Scintillator | | |
|---|---|---|---|---|---|---|---|
| | | | Rotem | Automess | Organic | CsI (Tl) | BGO |
| A | 0.33 ± 0.06 (±18%) | 0.36 ± 0.11 (±30%) | 0.37 ± 0.17 (±46%) | 0.31 ± 0.20 (±64%) | 0.41 ± 0.04 (±9.8%) | 0.41 ± 0.11 (±27%) | 0.42 ± 0.06 (±14%) |
| B | 1.04 ± 0.14 (±13%) | 0.99 ± 0.20 (±20%) | 0.90 ± 0.27 (±30%) | 0.96 ± 0.26 (±27%) | 1.21 ± 0.09 (±7.4%) | 0.98 ± 0.17 (±17%) | 1.07 ± 0.10 (±9.3%) |
| C | 3.03 ± 0.24 (±7.9%) | 2.72 ± 0.38 (±14%) | 3.07 ± 0.64 (±21%) | 3.04 ± 0.31 (±10%) | 3.36 ± 0.26 (±7.7%) | 2.99 ± 0.67 (±22%) | 3.29 ± 0.21 (±6.4%) |

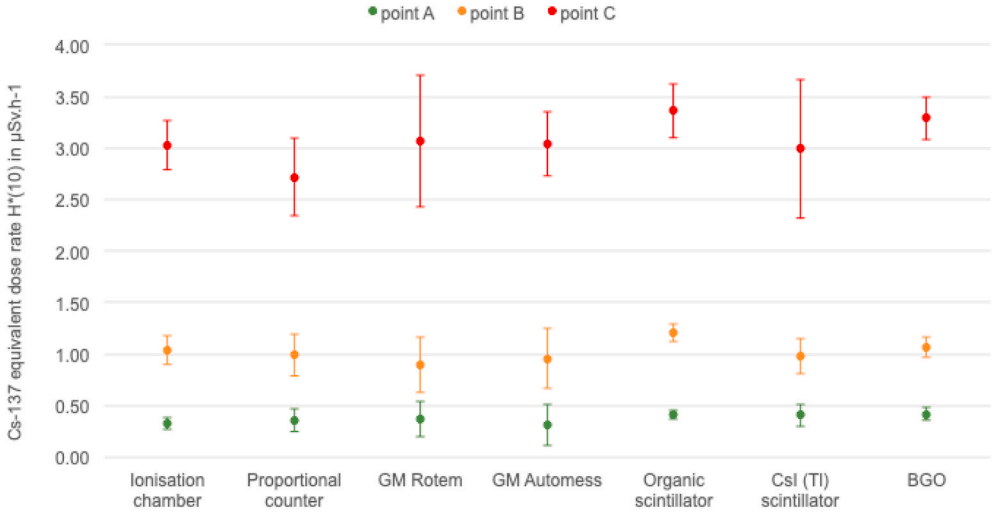


**Fig. 7.** Cs-137 equivalent dose rate H*(10) for the points A, B and C from the different equipment used. The error bars represent the expanded uncertainty (coverage factor 2).

- The mean values found for all three measurement points, taking the uncertainty bands into account, are very consistent;
- No significant difference is found between the results provided by tools that work outside their operating dose or energy ranges and tools that work within their ranges;
- No significant difference is found between the results provided by tools calibrated in terms of exposure dose or dose rate and tools calibrated in terms of ambient dose equivalent H*(10);
- The organic and the BGO scintillators tend to provide higher mean values compared to the other detectors but the difference is not significant and cannot be explained in terms of efficiency as the first one has nearly flat energy response and the BGO measurement has been corrected for its energy response (see Fig. 5).
- The organic scintillator, the BGO and the ionisation chamber provide the smallest expanded uncertainty, especially for the low dose rate point, and
- The GM Rotem equipment has a relatively high response time for small changes (30 s) and this value could be a cause of the high uncertainties observed for this equipment if this time had not been respected between consecutives measurements.

Finally, it should be pointed out that two of the most significant challenges of these measurements: the restrictive environment, with radiation arriving from all points from the biological shield and the time needed, not only to perform the measurements, but also to stabilize the equipment between measurements, do not seem to have affected the quality of the results obtained.

### 4.2. Total gamma measurements

The results of the total gamma measurements, expressed as Cs-137 equivalent Bq cm$^{-2}$ of the detector, are shown in Table 5. The values reported correspond to the arithmetic mean of the 25 single measurements for each of the points A, B and C. The reported expanded uncertainty (coverage factor 2) only consists of the standard deviation of the values measured. In addition, in this case, no reference value is available to compare the results with each other. The results are graphically represented in Fig. 8.

One can instantly observe the immense absolute dispersion between the mean values for the various measurement equipment and each specific data point. However, Fig. 8 also clearly shows that the relation between points A, B and C seems to be relatively stable comparing the various detectors. The main reasons for the absolute dispersion are:

- The different detector responses as a function of energy (see Fig. 6). All the detectors were calibrated locally at the SCK CEN facilities by

**Table 5**
Total gamma measurement results (Cs-137 equivalent Bq.cm$^{-2}$) for the various measurement equipment used and the expanded uncertainty (relative uncertainty between brackets, k = 2).

| | Proportional counter | | Scintillator | | | | | |
|---|---|---|---|---|---|---|---|---|
| | Berthold | Thermo Scientific | ZnS Berthold | ZnS + Organic Nuvia | Organic Nuvia | NaI (Tl) | $LaBr_3$ | BGO |
| A | 67.6 ± 8.1 (12%) | 12.7 ± 1.9 (15%) | 25.3 ± 4.0 (16%) | 8.48 ± 0.90 (11%) | 28.1 ± 1.8 (6.4%) | 188 ± 66 (35%) | 31.5 ± 1.4 (4.4%) | 56.4 ± 5.6 (9.9%) |
| B | 178 ± 13 (7.1%) | 34.6 ± 5.1 (15%) | 87.3 ± 7.4 (8.4%) | 23.1 ± 2.5 (11%) | 90.2 ± 3.1 (3.4%) | 654 ± 229 (35%) | 111.7 ± 1.1 (0.98%) | 177 ± 11 (6.2%) |
| C | 508 ± 31 (6.1%) | 98 ± 14 (14%) | 275 ± 15 (5.3%) | 62.9 ± 6.7 (11%) | 248 ± 13 (5.3%) | 1918 ± 671 (35%) | 333.3 ± 2.1 (0.63%) | 525 ± 19 (3.6%) |

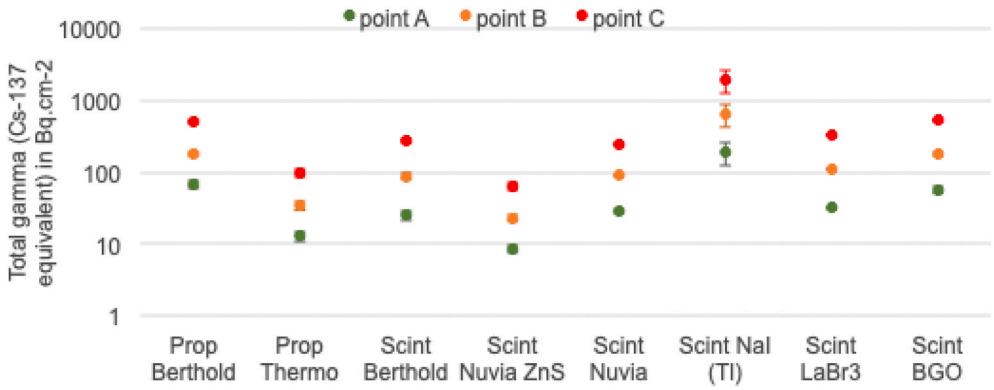


**Fig. 8.** Total gamma expressed as Cs-137 equivalent in Bq.cm$^{-2}$ for the points A, B and C from the different equipment used (logarithmic scale). The error bars represent the expanded uncertainty (coverage factor 2).

using a Cs-137 point source. However, considering the information provided in Fig. 4, most of the gamma emissions from the biological shield have an energy lower than 500 keV; and hence the different response of each detector as a function of photon energy matters (see Fig. 6). For example, most detectors show a homogeneous and energy independent response (normalized values with respect to Cs-137 are between 0.4 and 1.6 in the 600–1400 keV energy range). However, the NaI(Tl) scintillator shows a response value between 2 and 8 for energies below 500 keV. Therefore, the results provided by using this detector should be necessarily higher than the results provided by the others.

- The combination of the various detector shapes and sizes (see Table 2) with the calibration procedure using a point source and contact measurement. Geometrically, there is a large difference between calibrating a cylindrical shaped detector at the end cap (small solid angle) with a point source in contact and applying the same procedure for a rectangular surface detector (nearly 2π efficiency). The real source (biological shield) has infinite dimensions compared to those of the detectors and the activity distribution in X-Y direction can be considered as homogeneous. Nevertheless, the activity distribution in depth is a typical activation profile resulting in different self shielding for different photon energies.

Additional reasons for the large dispersion of the mean values identified are the following:

- Incorrectly taking beta radiation into account: the three surface contamination monitors (ZnS Berthold, Organic + ZnS Nuvia and Organic Nuvia) have comparable surface sizes. The only large difference is that, in principle, the three scintillation detectors are able to detect beta radiation. However, the Organic Nuvia monitor is equipped with an aluminium cover to prevent from beta radiation detection and the ZnS Berthold detector was additionally shielded from beta radiation during the measurements and the calibration. However, this was not the case for the Organic + ZnS Nuvia detector. The latter could detect beta radiation both during the measurement and during the calibration, since the calibration source was also emitting beta radiation. This seriously complicates the interpretation of the results from the Organic + ZnS Nuvia detector. As stated before, all other detectors are shielded by their own structure, housed in aluminium.
- Deviation of the agreed calibration procedure: two teams did not exactly follow the agreed calibration procedure. The results for the Thermo Scientific proportional counter were corrected by modelling the real measurement setup using MCNP 5. Also, for the BGO detector corrections for the real measurement setup were applied, using PENELOPE modelling instead of MCNP.

The high-energy range of some detectors (e.g. Thermo proportional counter and MIRION inorganic scintillator NaI(Tl), up to 4400 and 1500 keV, respectively) does not matter in this exercise due to the small percentage of gamma emissions of the biological shield at those high energies (See Fig. 6).

Other possible minor sources of data dispersion, such as energy operational range, stabilization times, etc., could not be evaluated in this exercise due to the great disparity of results presented.

All these facts, lead us to consider that the results in total gamma cannot be compared from the point of view of the absolute values obtained. However, since the relations between points A, B and C seems to be relatively stable, we compared the ratios A/B and A/C for the various detectors. The results are presented in Fig. 9.

The ratios are more consistent considering the error bars. Discarding the Organic + ZnS Nuvia results due to the additional uncertainty due to beta, the A/B ratio for the scintillators seems to be consistent. The proportional counters seem to give similar but larger values (potentially due to an effect of beta radiation or low energy photons). The $LaBr_3$(Ce) detector results present the lowest uncertainty, followed by the Organic Nuvia detector, Como 300.

In view of the benchmarking exercise goal and the mapping of the inner surface of the biological shield, the use of the NUVIA organic scintillator applying a 15 s integration time results in an expanded uncertainty for the repeatability/reproducibility between 3.4% and 6.5%. This is a similar result to the organic scintillator, used for dose rate measurements (see Table 4). A separate validation study showed that the uncertainty of the linearity within the count rate range in the biological shield is negligible. Using the $LaBr_3$(Ce) detector and applying a measurement time of 30–45 s would considerably improve the uncertainty at the higher and medium activation locations, but only slightly improve the uncertainty at the low activated locations.

### 4.3. *Gamma spectrometry measurements*

Table 6 lists the results for the parameters obtained using gamma spectrometry and modelling for the various detectors and calculations tools. The parameters to be reported were defined for the following reasons:

- Depth where the most abundant radionuclides, Ba-133 and Eu-152, (and the combination) reach a certain activity concentration: those are the locations where the end stage of the materials change from conditional to unconditional release. These parameters are closely connected to the sub-objectives of this exercise.
- Eu-152/Eu-154 ratio and Cs-137 surface contamination: feasibility to quantify trace radionuclides being present. The presence of Cs-137 traces are probably originating from remaining small pieces of the

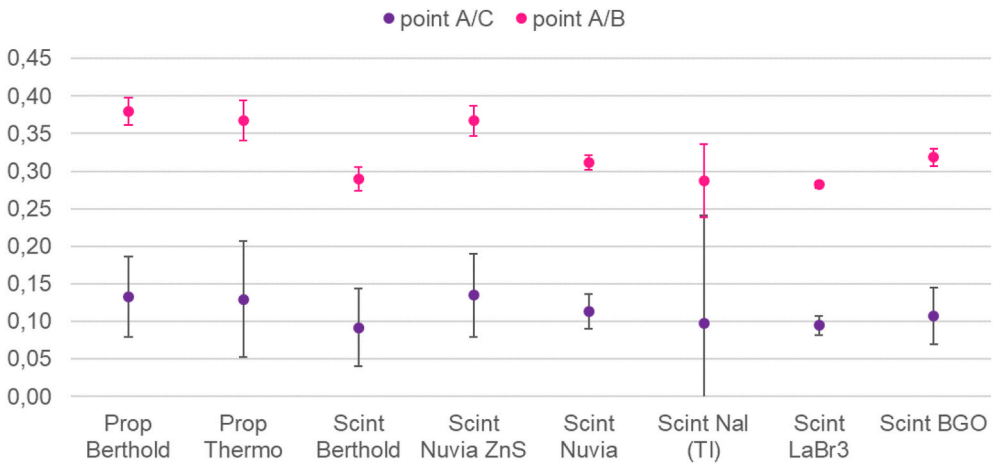


**Fig. 9.** Total gamma ratios for points A/C and points A/B for the detectors used. The error bars represent the expanded uncertainty (coverage factor 2).

**Table 6**
Parameter values obtained using gamma spectrometry for each of the detectors and modelling.

| Detector type | Scintillator | Semi-conductor | | | | |
|---|---|---|---|---|---|---|
| Detector model | $LaBr_3$(Ce) - | CZT [3] | HPGe B2830 | HPGe GL2020 | HPGe GX4018 | HPGe BE3830 |
| Energy resolution | Medium | Medium | High | High | High | High |
| Calibration and modelling | MCNP6.1 | PENELOPE MC | ISOCS | MCNP5-1.60 | ISOCS | ISOCS |
| Depth (cm) where Ba-133 $\leq$ 0.1 Bq.g$^{-1}$ | 56 ± 1.92 | 51 ± 3.2 | 50 | 57 ± 1.2 | 57 ± 0.1 | 55 ± 0.6 |
| Depth (cm) where Eu-152 $\leq$ 0.1 Bq.g-1 | 40 ± 1.9 | 37 ± 4.8 | 35 | 45 ± 1.8 | 37 ± 0.4 | 38 ± 1.4 |
| Depth (cm) where $\Sigma$(Ba-133/0.1 + Eu-152/0.1) $\leq$1 Bq.g$^{-1}$ | 57 ± 1.9 | 52 ± 5.8 | 52 | 59 ± 2.2 | 58 ± 0.4 | 57 ± 1.6 |
| Activity Eu-152/Eu-154 | 30 ± 16 | 1.8 ± 2.10 | 16 ± 0.24 | 13 ± 2.6 | 17 ± 1.8 | 18 ± 0.4 |
| Cs-137 surface cont (Bq.cm$^{-2}$) | 0.368 ± 0.594 | 0.883 ± 0.888 | 2.040 ± 0.006 | 0.74 ± 0.44 | 0.3440 ± 0.0002 | 0.3950 ± 0.001 |

liner. The distribution is therefore more surface oriented but not homogeneous in X-Y direction.

When mentioned in Table 6, the uncertainties (coverage factor 2) are only related to the 2 sigma uncertainty on the peak area calculation of the photo peaks, and combined when two radionuclides are combined. Of course, the uncertainty on the peak area calculation is usually negligible compared to other potential uncertainties. For the modelling, every participant used the same activation profile and chemical composition and density of the concrete. Differences found for the various systems used are therefore mainly related to the properties of the detector (e.g. resolution), the transcription of the complete measurement geometry (detector, setup, source) into a model and the calculations using a specific software based on Monte Carlo.

We observe the following for the most abundant radionuclides:

- The results obtained for the three parameters are fairly consistent.
- The results for the four high resolution HPGe detectors are nearly the same. The two most comparable systems (GX4018+ISOCS & BE3830+ISOCS) give approximately the same results. The GL2020+MCNP5 provides a slightly different result for the Eu-152 depth, but this has a limited effect on the sum (Ba-133+Eu-152). The B2830+ISOCS (Falcon), which was not shielded, produces a different result, mainly due to the Ba-133 quantification.
- The medium resolution inorganic scintillator detector $LaBr_3$(Ce) also provides the same results as the high resolution HPGe detectors for these most abundant radionuclides.
- The results for the medium resolution detector and small CZT differ from the high resolution detectors, and the LaBr3(Ce), but differences are considered to be relatively small taking the complex gamma spectra into account.

For the trace radionuclides, we notice that:

- The results for Eu-154 compared to Eu-152 are still reasonably consistent for the four high resolution HPGe detectors. However, the values obtained by medium resolution detectors are clearly different from those reported by HPGe detectors.

When using medium or low-resolution detectors almost all the Eu-152 gamma-peaks have some interference with the Eu-154 gamma peaks. However, the Eu-152 peak of 1408 keV (21%) has only very minor interferences and then it can be resolved with sufficient precision to estimate the activity of this radionuclide. However, the case of Eu-154 is more complicated, as among its gamma-peaks, the only one almost free of interference from Eu-152 is the 1274 keV (35%); unfortunately, it interferes with Co-60, which is also present in the biological shield.

Thus, the only detectors able to discriminate Eu-152 from Eu-154 when they are present in dissimilar concentrations are the HPGe, due to its high resolution.

- Regarding Cs-137 surface contamination activity, again, the two most comparable systems (GX4018+ISOCS & BE3830+ISOCS) give very similar results. Despite the result of the medium resolution LaBr3(Ce) detector being quite identical its uncertainty much higher.

The reason for the extreme value found with the Falcon (B2830+ISOCS) is most likely due to the lack of detector shielding and the presence of contamination at the pit below the detector. There is no obvious explanation for the different surface activity concentration found for Cs-137 using the CZT + PENELOPE and the GL2020+MCNP5 on the one hand and the $LaBr_3$(Ce)+MCNP5, the GX4018+ISOCS and the BE3830+ISOCS on the other hand. The most probable reason is that although all detectors in theory used the same distance detector-wall (30 cm) and collimation (90°), in practice the surface seen by the detectors (and the amount of remaining liner pieces with Cs-137 traces) could be different.

The on-site gamma spectrometry benchmarking exercise shows that results for high-resolution detectors are generally very consistent, when using proper shielding. Results for medium resolution gamma spectrometry can still be noteworthy comparable for the main radionuclides present. There are of course obvious limits in terms of quantification of lower concentration radionuclides and trace elements due to their medium resolution that does not allow discrimination nearby gamma ray energies and the small size used in the case of CZT detectors.

The exercise also shows that the various modelling tools used provide consistent results. Nevertheless, there is no denying that such a benchmarking exercise would be pretty much impossible without providing the crucial information such as the activation profiles for the individual radionuclides to the participants (besides the essential data of the concrete chemical composition and density). Sampling and analysis in the lab still remains indispensable for rather complicated situations like the one given in this biological shield.

## 5. Conclusions

This paper reports on the results of the on-site benchmarking exercise of the BR3 biological shield. We described the measurements performed, some of the properties and measurement parameters of the different measurement equipment being used and its applicability in view of accomplishing the general exercise goal or one of its three sub objectives. A total of seven organisations performed three types of on-site measurements using their own equipment. Constraints were mainly related to typical nuclear safety issues (radiation & contamination hazards) but above all to access limitations and classical safety hazards.

The mean values of all dose rate measurements performed, using a large variety of measurement equipment (different types of gas detectors and scintillators) not always calibrated in terms of ambient dose equivalent H*(10) and sometime measuring outside their operational range, are very consistent. Nevertheless, the uncertainty on a single measurement can be very large for certain types of detectors. In view of using the results of this type of measurements to map the inner surface of the biological shield the most appropriate equipment tested might be the organic scintillator, the BGO or even the ionisation chamber as they show smaller relative uncertainties. For the ionisation chamber, the uncertainty on the very low dose rates might, however, already become slightly large.

The total gamma measurements were more difficult to compare due to high variety of detectors being used (two different proportional counters and six different scintillators detectors, some of them being gamma probes and other surface contamination monitors) and the limitation of the calibration procedure, which was not always strictly followed by participants. For mapping the inner surface of the biological shield, the most appropriate equipment tested might be the $LaBr_3$(Ce), the thick organic scintillator or the BGO. Other equipment tested might be still be appropriate using adapted data acquisition integration times, depending on the allowed maximum uncertainty at the lower activities (measurement point A). The expanded uncertainty using the thick organic scintillator ranges from 3.4% to 6.4%. This is nearly exactly the same as for the organic scintillator used for the dose rate measurements. The uncertainties can be reduced using a $LaBr_3$(Ce) and, or possibly, combining this with shielding. In practice, this might be, however, a little bit too complex.

These in situ total gamma measurements, on a given area, are dependent on several factors: the geometry of the area, the distribution of gamma activity, the background radiation and the measurement procedure (monitor-area distance and size and type of the probes used). Therefore, the total gamma measurements can be used as a secondary parameter in a relative way. Trying to compare absolute values from different measurement probes and methodologies is too complex and makes no sense in view of decommissioning objectives.

The on-site benchmarking exercise for the gamma spectrometry showed very consistent results for the high resolution measurement equipment and the main parameters to be determined. The results from the medium resolution equipment and the main parameters were a little bit different, but still remarkably comparable taking the complex gamma spectrum into account. It is, however, clear that the in-situ gamma spectrometry can be an interesting technique to apply, but it cannot fully replace sampling and analysis in the lab for this facility.

The overall BR3 biological shield characterisation program consisted of total gamma measurements at the inner surface of the biological shield (secondary data) using the thick organic scintillator NUVIA and gamma spectrometry measurements on drill core samples (primary data). Modelling and interpretation of all data acquired is still ongoing and will be published in the future. Preliminary calculations show that the uncertainty on the total gamma measurements will be pretty small compared to the uncertainties on modelling the 3D specific activity distribution map.

## Declaration of competing interest

The authors declare that they have no known competing financial interests or personal relationships that could have appeared to influence the work reported in this paper.

## Acknowledgements

INSIDER is a EU Horizon 2020 project and received funding from the Euratom Research and Training Programme 2014–2018 under grant agreement No 755554.

## References

Amgarou, K., Herranz, M., Csöme, C., Aspe, F., 2018. Inventory of Existing Methodologies for Constrained Environments. INSIDER deliverable 5.1. https://app.lgi-consulting.org/mso/ecm/insider-ecm-file-17549.

Aspe, Frédéric, Idoeta, Raquel, 2019. Classification and Categorization of the Constrained Environments. INSIDER Deliverable D5.2. http://www.insider-h2020.eu.

Aspe, Frédéric, Idoeta, Raquel, Auge, Gregoire, Herranz, Margarita, 2020. Classification and categorization of the constrained environments in nuclear/radiological installations under decommissioning and dismantling processes. Prog. Nucl. Energy. https://doi.org/10.1016/j.pnucene.2020.103347.

Boden, S., Cantrel, E., 2007. Pre-decommissioning radiological characterization of concrete. In: Proceedings of the 11th International Conference on Environmental Remediation and Radioactive Waste Management ICEM 2007, vol. 1. Bruges, Belgium, 2007.

Boden, S., Rogiers, B., Dadoumont, J., Noynaert, L., Garcia-Miranda, M., Roudil, D., 2018. R&D within the BR3 PWR Decommissioning Project, DEM 2018, Avignon, France.

Boden, S., Rogiers, B., Verstrepen, G., Mangelschots, N., Broeckx, W., 2019. WP3 Sampling Strategy - Sampling Plan for Use Case 2: BR3 Bioshield. Deliverable 3.5. http://insider-h2020.eu/wp-content/uploads/2019/04/INSIDER-D3.5_Sampling-plans-for-use-case-2.pdf.

Broeckx, W., Rogiers, B., Mangelschots, N., Vandyck, R., Verstrepen, G., Boden, S., 2020. INSIDER UC2: the BR3 Biological Shield: Preliminary Results and Future Work, INSIDER Mid-term Workshop. Bilbao, 2019, EPJ-N 190019.

GfdT, 2002. Gebrauchsanweisung für die Teletectorsonden 6150AD-t, 6150AD-t/H, 6150AD-t/E, Automess, 13.09.2002.

IAEA, 1998a. Radiological Characterization of Shut Down Nuclear Reactors for Decommissioning Purposes. International Atomic Energy Agency, Vienna. IAEA technical report series n. 389.

IAEA, 1998b. Characterization of Radioactively Contamined Sites for Remediation Purposes. International Atomic Energy Agency, Vienna. IAEA-TECDOC-1017.
IAEA, 2004. International Atomic Energy Agency, Application of the Concept of Exclusion, Exemption and Clearance – Safety Guide. IAEA Safety Standards Series No. RS-G-1.7, Vienna.
IAEA, 2007. Strategy and Methodology for Radioactive Waste Characterization. IAEA-TECDOC-1537 International Atomic Energy Agency, Vienna.
INSIDER, 2017. The INSIDER Project. http://insider-h2020.eu/.
Knoll, G.F., 2010. Radiation Detection and Measurement, fourth ed. Ed.Wiley.
NEA, 2013. Radiological Characterisation for Decommissioning of Nuclear Installations.
NEA, 2017. Radiological Characterization from a Waste and Materials End-State Perspective, Practices and Experiences.
Peerani, P., Boden, S., Crozet, M., Zanovello, F., Herranz, M., Serrano, R., Roudil, D., 2018. Design of the Benchmarking Exercise. Deliverable 2.5. http://www.insider-h2020.eu.
Steffen, M., 2020. Eichstelle - Paul Scherre Institute (PSI), Private Communication, 13.02.20.
WNA, 2019. The World Nuclear Association. https://www.world-nuclear.org/nuclear-basics/glossary.aspx.